BMC Biology

RESEARCH

Open Access

Chromosome-level genome assembly and Oligo-FISH confirmation of chromosome models for the Tasmanian snow skink *Carinascincus ocellatus* (Scincidae, Eugongylinae)

Paul A. Saunders[1,2*], Francisco M. C. Sassi[3,4], Marcelo B. Cioffi[5], Oleg Simakov[6], Christopher P. Burridge[1], Tariq Ezaz[3] and Erik Wapstra[1]

Abstract

Background Skinks (Scincidae) are one of the most diverse and ecologically versatile lizard families, making them key models for studying major evolutionary transitions including viviparity, limb reduction, and shifts between modes of sex determination. Despite their diversity and research potential, skinks remain underrepresented in genome databases, limiting comparative studies and our ability to investigate the genetic foundations of their evolutionary diversity.

Results We generated a high-quality chromosome-level genome assembly for the Tasmanian snow skink, *Carinascincus ocellatus*, using PacBio long-read sequencing and Hi-C scaffolding. We validated the accuracy of chromosome models in this genome using an innovative application of Oligo-FISH, designing thousands of short probes directly from the genome assembly and hybridizing them to a single *C. ocellatus* metaphase slide. This single-step approach provides direct and independent cytogenetic validation of all 15 chromosomes in the assembly, including microchromosomes, which are broadly recognized as more susceptible to misassembly. We further demonstrate the approach's cross-species utility through comparative cytogenomics and in silico probe alignment to multiple other skink genomes, highlighting its potential for multi-genome validation and comparative analyses.

Conclusions Our study establishes *C. ocellatus* as a genomic model for skinks and positions Oligo-FISH as a scalable, cost-effective, and broadly applicable approach for chromosome-level genome validation. By applying it across species, we demonstrate the method's potential to support more reliable genome reconstruction and comparative genomic analyses.

Keywords Genomics, Cytogenetics, Reptile genome, Oligonucleotide probes, Microchromosomes, Scincidae

*Correspondence:
Paul A. Saunders
paul.alan.saunders@gmail.com
Full list of author information is available at the end of the article

Background

Skinks (family Scincidae) account for nearly a quarter of all described lizard species, making them one of the most species-rich families of squamates (over 1750 species identified). They have a near-global distribution, thrive in many habitats, and exhibit a remarkable diversity in body size, limb morphology, reproductive cycles and modes, and social structures [1]. This diversity makes them prime models for investigating key evolutionary processes including the evolution of viviparity and sociality [2, 3], limb reduction and loss [4], and transitions in sex determination [5]. Notwithstanding their ecological and evolutionary significance, skink genomes are poorly represented in genomic resources, with assemblies accessible for just 1% of species (Fig. 1), much lower than other lizards such as lacertids (7.7%) and agamids (2.9%), which are already significantly underrepresented in genomic databases relative to birds and mammals (exceeding 12%). This limits our ability to study skink—and more broadly squamate—diversity and evolutionary transitions. Consequently, adding genomic resources for skinks is essential for realizing their potential to increase our understanding of significant evolutionary transformations at the molecular level.

An emerging model skink in evolutionary research is the Tasmanian snow skink, *Carinascincus ocellatus* (Scincidae, Eugongylinae). This is a small (adult mass: 3–10 g) viviparous lizard endemic to Tasmania. Research on this species has greatly benefited from a long-term monitoring program (25 + years) of life-history traits at the extreme altitudinal and thermal limits of its range. This has supported studies into key evolutionary processes including developmental plasticity, aging and senescence, adaptation to high altitude, and sex determination, with a particular focus on how environmental factors drive these traits [6–9]. A reference genome for *C. ocellatus* would not only enhance ongoing research on this species but also provide a powerful model for investigating the genetic mechanisms underlying major evolutionary transitions in skinks and reptiles more broadly, particularly those related to sex determination, developmental responses to environmental variation, and life-history evolution. The current gold standard in the development of reference genomes is the assembly at a "chromosome-level," where each chromosome is represented by one contiguous sequence, i.e., a chromosome model. Chromosome-level reference genomes support the investigation of functional, comparative, and population genomics both within and among species. Assemblies of high contiguity, high quality, and reliability are crucial for studying chromosome-scale evolution or investigating structural variants, both of which have far-reaching applications in fields ranging from comparative genomics [10–13] to conservation [14–17]. Chromosomal-level reference genomes are typically achieved via the assembly of large contiguous sequences using

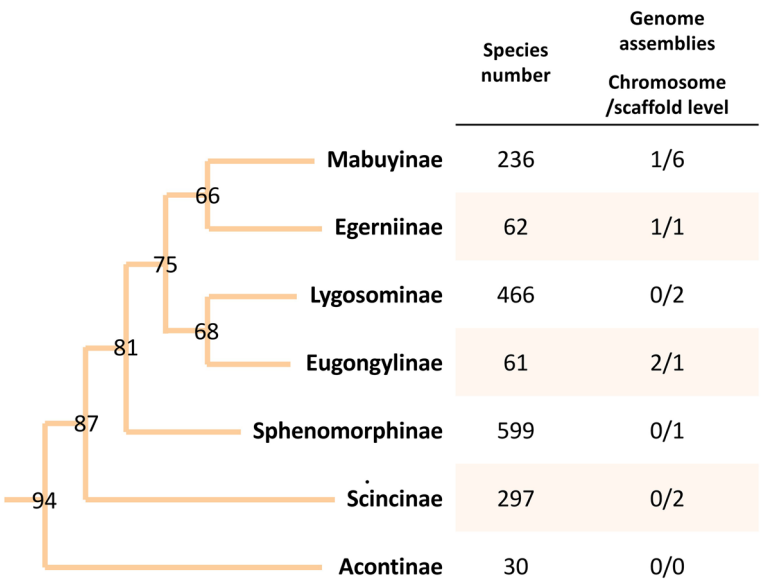

Fig. 1 Dendrogram illustrating the relationships among skink subfamilies, along with number of species and genome assemblies (chromosome or scaffold level) available in each subfamily. Dendrogram made following [75]. Divergence times displayed on nodes: median time from timetree.org (in million years). Classification and number of species from [76] and Reptile Database 2024. Genome assemblies accessed on NBCI in March 2025. Additional file 2: Table S1 summarizes information regarding the available skink genomes, including assembly level, chromosome number, and N50

long-read sequencing, followed by the scaffolding of the assembled sequences into chromosome models using conformation capture technology (e.g., Hi-C), which uses chromosome interactions to gain information on long-range contiguity [18].

While the combination of long-read sequencing and Hi-C has proven effective in producing reliable chromosome-level assemblies for many organisms [19], some genomes remain challenging to assemble this way. Potential deficiencies include large-scale misassemblies, resulting in incorrect identification of chromosome boundaries and/or assignment of certain sequences to the wrong chromosomes [20–22]. This is an issue known to occur in genomes containing microchromosomes. These small chromosomes (usually < 30 Mb) found in many vertebrates tend to cluster in the center of nuclei and show a high degree of inter-chromosomal chromatin interaction [23, 24]. This makes microchromosomes challenging to distinguish during Hi-C scaffolding, which is designed to join genomic sequences based on the frequency of physical contacts between them. Assembly challenges related to microchromosomes have been reported in birds, lizards, and snakes [25–27].

To confirm that chromosome models in a genome assembly are accurate (and thus reliable for comparative genomics), bioinformatics-based chromosome assemblies should ideally be independently verified [22, 28, 29]. Karyotype counts can be used to validate that the correct number of chromosome models has been assembled [30, 31], while in silico detection of telomeric repeats at the end of chromosome models can provide support for their complete assembly. However, both methodologies could fail to recognize significant inter-chromosomal misassemblies (e.g., ref. [32]), and hence fall short of definitive validation of chromosome models. Several approaches have emerged to independently validate chromosome models and link genome assemblies to physical chromosomes. For instance, individual chromosomes can be isolated via flow sorting or microdissection, sequenced and mapped to a reference genome, or assembled de novo individually (ChromSeq; [33, 34]). The two most widely used approaches for independent validation of genome assemblies are linkage mapping and fluorescence in situ hybridization (FISH). Linkage mapping is highly effective [35], but is restricted to species with short generation times and/or that are easy to breed [36]. FISH, a cytogenetic method for physically observing the location of known genetic markers on chromosomes, has been used to identify and correct misassemblies in the tomato genome [32], to assist scaffolding of fragmented bird genomes [37, 38], and more recently to validate Hi-C scaffolding in a turtle genome assembly [21]. These studies relied on pre-published FISH analyses, or a cumbersome, labor-intensive investigation involving hundreds of hybridizations of pre-existing Bacterial Artificial Chromosome (BAC) probes. In species lacking pre-existing probes, the approach becomes even more costly and time-consuming, making it difficult to scale up. The difficulty of implementing linkage mapping and FISH approaches and applying them consistently across species represents a current limitation for the chromosome-level validation of genome assemblies.

The increasing number of species with fully sequenced genomes has initiated a new phase in the chromosome-to-genome mapping process via the development and use of oligonucleotide-based probes, often referred to as "Oligo-FISH." This approach entails identifying several oligos that are unique to a chromosomal region or whole chromosomes in silico using specialized pipelines [39]. The oligonucleotides may then be synthesized, tagged as probes, and hybridized in situ to metaphase chromosomes. Oligo-FISH has been widely employed to study chromosomes in plants in recent years [40–44]. However, this approach has only been applied in two studies involving vertebrate species: Huang created oligo probes for a subset of the chicken chromosomes (nine dot chromosomes) to verify their indexing [45], while Poisson et al. used Oligo-FISH probes to assist scaffolding of the fragmented reindeer (*Rangifer tarandus*) genome assembly [46].

In this paper, we assemble a high-quality chromosome-level genome for the Tasmanian spotted snow skink *C. ocellatus* using PacBio and Hi-C data and validated all 15 chromosome models using Oligo-FISH. Unlike previous vertebrate applications that targeted only a subset of chromosomes or was designed to enhance scaffolding, our study applies Oligo-FISH as a post hoc genome-wide validation method, validating all chromosomes models simultaneously on a single metaphase slide. Hence, this genome stands as the most comprehensively validated skink genome to date, setting a benchmark for future genomic studies in this lineage. We further demonstrate the broader applicability of this approach by hybridizing the same probe set to metaphase spreads of other skink species and aligning the oligos in silico to additional skink genome assemblies spanning ~ 75 million years of divergence. These results reveal notable karyotype conservation across the Eugongylinae and highlight the potential of Oligo-FISH as a scalable method for cross-species genome validation and comparative genomics using a single probe set.

Results

Genome assembly and annotation

We assembled a chromosome-level male genome for *Carinascincus ocellatus* from Tasmania's Central Plateau

(41 51′S, 146 34′E). PacBio HIFI reads (36× coverage assuming a 1.5 Gb genome) were assembled using *Hifiasm*, producing a primary contig assembly composed of 82 sequences with a N50 of 98 Mb and a total length of 1.51 Gb. The genome shows a high level of BUSCO completeness with 97.7% of complete vertebrate universal single-copy orthologs identified (C: 97.7%, [S: 96.8%, D: 0.9%], F: 0.8%, M: 1.5%, n: 3354).

Contigs were assembled into scaffolds using Hi-C reads (40× coverage) and programs *Juicer* and *3DDNA*. Based on prior knowledge that *C. ocellatus* has a karyotype composed of 15 chromosome pairs (8 macro- and 7 microchromosomes [47, 48]), we used *Juicebox* to manually delimitate chromosome boundaries, yielding an assembly composed of 15 chromosome models (size range 14–287 Mbp), containing > 99.9% of all nucleotides (Fig. 2, Additional file 1: Fig. S1). Relative chromosome model length correlates with relative metaphase chromosome size, and smaller chromosome models display a greater GC content (44.9–48.0%) than larger chromosomes (42.6–44.8%; Additional file 1: Fig. S2), consistent with expectations [24].

We masked the genome using *Repeatmasker*, finding 46.34% of the genome composed of repeat elements (Additional file 1: Fig. S2, Additional file 2: Table S2). Telomeric repeats were identified at both ends of chromosome models except for 5, 9, 12, and 14, where they were found only at one end (Fig. 2B, Additional file 2: Table S3). Telomeric sequences were also found in the centromeric regions of the two largest macrochromosomes, in line with previous cytological observations [48]. We assembled genes with *Braker3*, identifying 31,312 transcripts for 26,690 gene models (Additional file 2: Table S4). Running *BUSCO* in protein mode suggests a 98.6% completeness of the annotation when compared to conserved single-copy vertebrate proteins (C: 98.6%, [S: 97.5%, D: 1.1%], F: 0.5%, M: 0.9%, n: 3354). Most transcripts (19,459, 62%) are fully supported by RNA and/or protein evidence (i.e., external evidence for start and stop codons and support for introns if present), 5594 transcripts (18%) have partial support, and 6259 (20%) are ab initio transcripts with no support and might represent false positives. Functional annotation of transcripts allowed us to confidentially transfer a functional annotation to 25,191 transcripts, most of which are genes with full or partial RNA/protein support (75% and 19%, respectively; Additional file 2: Table S4). Gene density is greater in microchromosomes (Additional file 1: Fig. S2). The mitochondrial DNA was assembled based on raw PacBio HIFI reads, resulting in a circular chromosome of 17,866 bp containing 37 genes.

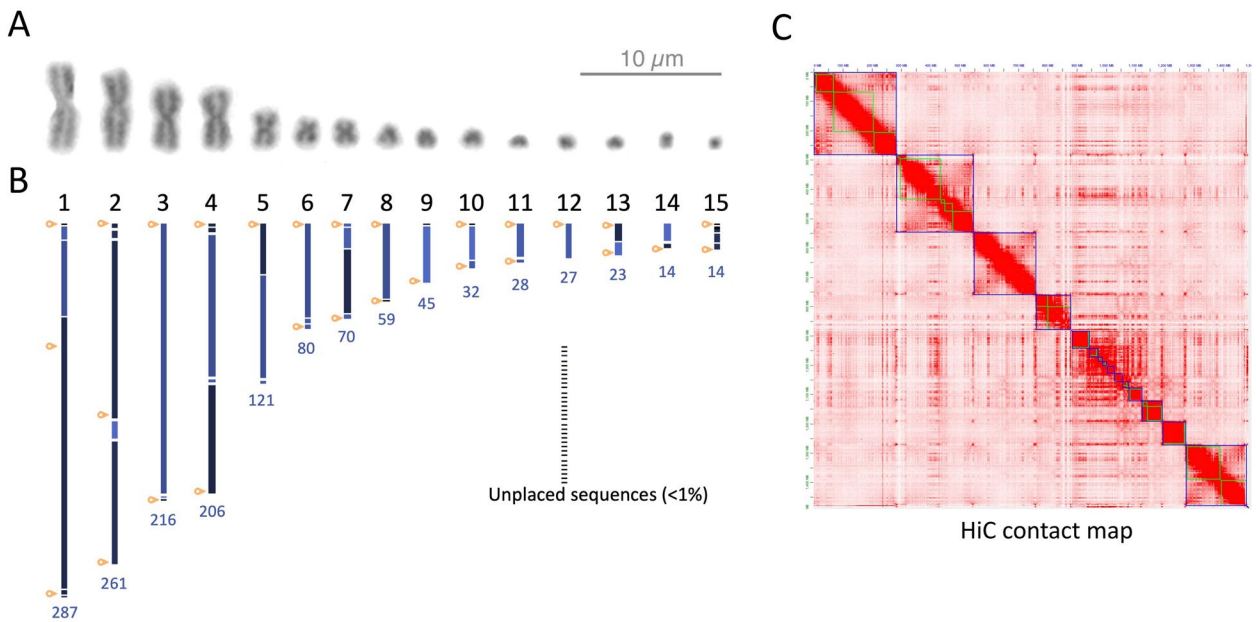

Fig. 2 Genome assembly for *Carinascincus ocellatus*. **A** *C. ocellatus* chromosomes, DAPI karyotype. **B** Sequences assembled into chromosomes from largest to smallest. Each segment is a contig. Number at top is chromosome number in assembly (largest to smallest scaffolds), and number at bottom is assembled sequence length (in Mbp). Pins show location of telomeric sequences detected (orange). **C** Hi-C contact map following manual chromosome boundary adjustment. Microchromosomes display a high degree of inter-chromosomal chromatin interaction. See Additional file 1: Fig. S1 for more details on delimitations of microchromosomes

Oligo-FISH chromosome indexing

Oligo-FISH chromosome indexing relies on mapping each chromosome model in the genome assembly to chromosomes on a metaphase spread in one single FISH experiment. For the genome of *C. ocellatus*, three oligo libraries were prepared. Each library contains oligos targeting 14 or 15 regions (nearly 2000 oligos/region). The regions were chosen so that when probes from each library are labeled with a different color fluorochrome (red/green/yellow), each chromosome should display a unique color pattern (Fig. 3A, Additional file 2: Table S5). Given the small number of chromosomes ($n=15$), all chromosomes were identified by a unique three-color barcode, with one central and two sub-telomeric probes (except for chromosome 15 with only one probe). In situ hybridization was conducted on *C. ocellatus* metaphases using the three oligo libraries simultaneously (Fig. 3B). After identifying isolated metaphases using DAPI staining, chromosomes were sorted by length, demonstrating a complete correspondence between the expected and observed color patterns for all 15 chromosomes (Fig. 3C). This confirms that the chromosome models in this genome assembly correspond with cytological interpretations, including chromosomal nomenclature.

Cross-species analyses

Fluorescent probes designed for *C. ocellatus* were hybridized to metaphases of the congeneric metallic snow skink *Carinascincus metallicus* and White's skink *Liophilis whitii* (different subfamily; Fig. 4A, B). Hybridization was successful on *C. metallicus* chromosomes, showing color patterns identical to that observed for *C. ocellatus*, suggesting no major chromosomal rearrangements following their divergence. Hybridization to *L. whitii* was unsuccessful—no signal could be distinguished from background noise (Fig. 4B).

Probe sequences were aligned in silico to the genome assemblies of Christmas Island blue-tailed skink *Cryptoblepharus egeriae* (subfamily Eugongylinae; same as *C. ocellatus*) and the chromosome-level assembly of the common blue tongue *Tiliqua scincoides* (subfamily Egerniinae; same as *L. whitii*). The mapping rate decreased from 100% in *C. ocellatus* to around 10% in *C. egeriae* and only 2% in *T. scincoides*. Successfully aligned probes were clustered in the expected regions according to whole genome alignments (Fig. 4C, Tables S6 and S7). This indicates that if hybridization is unsuccessful (e.g., in *L. whitii*), it is more likely due to sequence divergence rather than a lack of co-linearity.

Discussion

A reliable high-quality genome assembly for the Tasmanian snow skink

In this study, we present a high-quality genome assembly for the Tasmanian spotted snow skink, *Carinascincus ocellatus*. By combining PacBio Hifi reads and

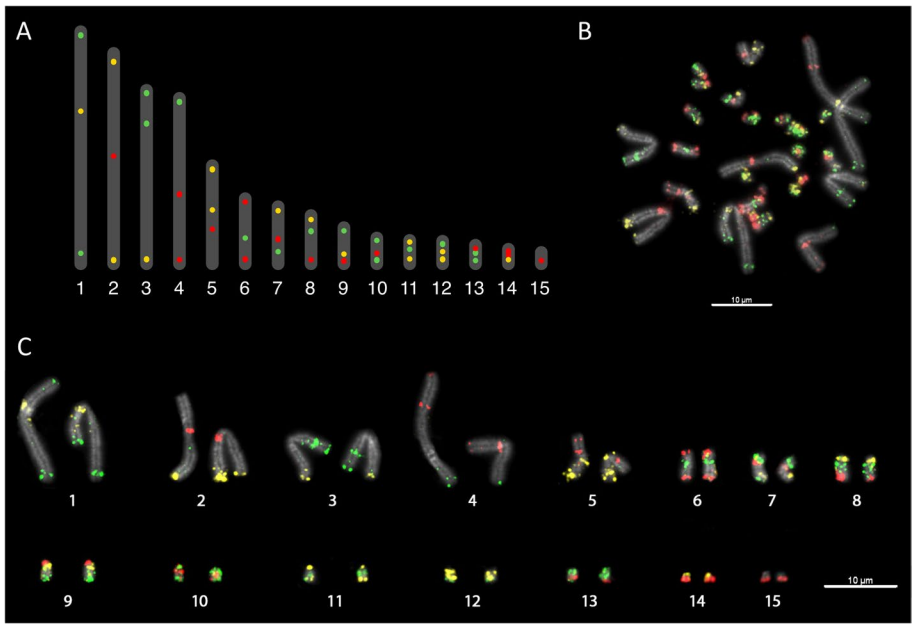

Fig. 3 Chromosome indexing to validate chromosome models. **A** In silico probe design: positions selected for probe design, with three oligo libraries shown in different colors: green/red/yellow (see Additional file 2: Table S5 for detailed location). Each chromosome model (1–15) has a unique probe combination. **B** Mapping of all probes to a *C. ocellatus* karyotype, raw image. **C** Isolation of each chromosome pair. See Additional file 1: Fig. S3 for DAPI chromosomes

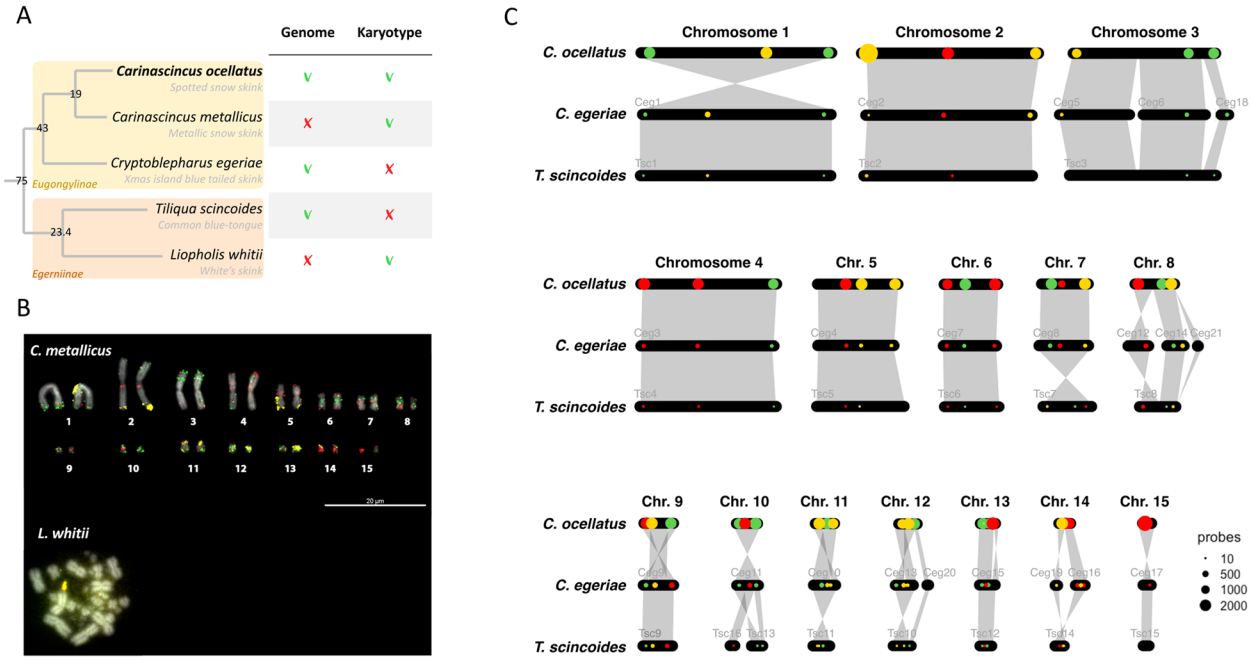

Fig. 4 **A** Phylogeny of the spotted snow skink and related species for which either metaphase-based karyotypes or genome assemblies were available at the time of our study. Numbers on nodes represent divergence time (median estimated divergence time in million years; time-tree.org). **B** Hybridization of *C. ocellatus* chromosome index probes on chromosome spreads of *C. metallicus* and *L. whitii*. **C** Alignment of chromosome models for *C. ocellatus*, *C. egeriae*, and *T. scincoides*. Each horizontal segment represents a chromosome model, sorted from largest to smallest based on *C. ocellatus* chromosomes. Whole genome alignments are shown in gray (see Additional file 2: Table S6 for details). Colored dots show the mapping density of probes along chromosomes in 1-Mbp windows (size of dots represents number of successfully mapped probes, minimum number of probes displayed: 10/Mb; Additional file 2: Table S7). Names above each *C. egeriae* and *T. scincoides* chromosome/fragment correspond to the sequence names in the genome assembly files

Hi-C data, we achieved a chromosome-level assembly with a contig N50 of 98 Mbp and high completeness (97.7% BUSCO score). This assembly is one of the most contiguous squamate genomes currently available in the NCBI database. As of now, only three chromosome-level assemblies have been reported in Scincidae (Fig. 1). Our genome metrics (assembly size, N50, GC content, repeat content) are comparable with other skink genomes (Additional file 2: Table S1) and demonstrate analogous disparities between macro- and microchromosomes: elevated GC content in microchromosomes and a higher density of repeat elements in macrochromosomes (Additional file 1: Fig. S2). The annotation yielded a protein-coding gene count with full support from RNA sequencing data and protein data (19,459 genes) comparable with the annotation of two other skink genomes [49, 50] and other squamates generally. In comparison to other chromosome-level genomes within Scincidae, the genome of *C. ocellatus* is distinguished by being comprehensively validated by cytogenetics (see ref. [51] for the advantages of integrating genomics with cytogenetics in the context of chromosomics).

Our motivation for cytogenetic validation stemmed from the inherent ambiguity observed in the Hi-C contact map, particularly for smaller chromosomes (Fig. 2, Additional file 1: Fig. S1). Despite the broad coverage of Hi-C data (40×), the boundaries of microchromosomes exhibited insufficient clarity—a problem previously documented in other vertebrate genome assemblies that include microchromosomes (e.g., birds, lizards, snakes [25–27]), and also visible in the published Hi-C maps of three other skink chromosome-level assemblies [49, 50, 52].

For the *C. ocellatus* genome, a series of measures were implemented to increase confidence in the bioinformatic delimitation of all chromosomes. Given the availability of karyotypes, Hi-C scaffolding was guided by prior knowledge of the diploid chromosomal number. After scaffolding, the genome was examined for telomeric repeats, which were detected at the termini of most chromosomal models (Fig. 2). A lack of repeats at one end of each of four chromosomes likely reflects an assembly limitation due to the highly repetitive nature of telomeric sequences rather than a biological feature. Similar gaps in telomere assembly have been reported in other chromosome-level

genomes (e.g., [49, 52]). A higher GC content and gene density was observed in smaller chromosomes, consistent with observations in other vertebrates [24], providing supportive (but not conclusive) evidence for the correct assembly of microchromosomes. In contrast, the use of a cytogenetic approach—validating the genome assembly at the chromosomal level using customized Oligo-FISH probes—provided a critical and independent validation of chromosome boundaries and overall genome integrity. This external validation establishes the genome of the Tasmanian spotted snow skink as a high-quality model for Scincidae, offering an optimal basis for comparative genomic studies among lizards, reptiles, and other vertebrate lineages.

Oligo-FISH for genome assembly validation

Several authors have emphasized the importance of external data to validate chromosome counts and structures in genome assemblies [19, 28, 29, 31, 51, 53], as errors can affect downstream analyses such as comparative genomics. However, such validation is rarely implemented due to practical challenges. Genetic mapping, while highly precise, is limited to species with short generation times and controlled breeding [35]. Similarly, FISH using BAC or gene probes is labor-intensive and typically restricted to species with pre-existing probes [21, 37, 38]. Oligo-FISH overcomes these limitations. Oligo probes are designed directly based on sequences of the genome assembly, so no additional genetic or cytogenetic data is necessary. Furthermore, oligo probes can be synthesized in parallel, avoiding the time- and labor-intensive cloning and screening steps required for BAC-FISH.

To validate the chromosome models of *C. ocellatus*, we created three oligo libraries, each labeled with distinct fluorochromes and targeting distinct sequences across 43 localities encompassing all 15 chromosome models. This produced unique color combinations that enabled us to anchor all chromosomes of the Tasmanian spotted snow skink genome (Fig. 3). The position of fluorescent spots perfectly matched the predicted position based on the in silico probe design, confirming that the chromosome models are correct and providing conclusive evidence that names given to chromosome models (chr1 to chr15) based on their size reflect the cytologic nomenclature. This significantly improves the reliability of the genome assembly. With three spots per chromosome, this experiment was designed mainly to detect interchromosomal misassemblies. The Hi-C contact map did not suggest any intra-chromosomal assembly discrepancies, but this could be confirmed with Oligo-FISH by preparing one or two supplementary libraries and labeling probes with additional fluorochromes (or a combination of fluorochromes) to increase resolution (number of loci per chromosome). However, increasing probe density might impair the differentiation of individual fluorescent signals (5 Mb is the minimum recommended distance between oligo probes for independent signals).

The number of libraries required during Oligo-FISH to validate a genome will depend mainly on (i) the chromosomal number in the karyotype and (ii) the desired resolution. Similar to previous methodologies, chromosome indexing will pose more difficulties in genomes with many chromosomes and/or small chromosomes; yet it remains feasible with enough resources. We believe that the decreased resolution of chromosomal indexing using Oligo-FISH (compared to genetic mapping or BAC-FISH) is considerably offset by its simplicity of execution, time efficiency, cost-effectiveness, and broader application. It is noteworthy that by precisely targeting unique sequences Oligo-FISH is particularly suitable for species with high repetitive content or polyploids, where chromosomal mapping is often considered challenging [54, 55].

Cross-species chromosome indexing

Oligo-FISH probes may be used beyond the targeted species. This was first illustrated in *Solanum*, where probes designed to barcode the potato karyotype were also effectively hybridized in six additional congeners, including tomato and eggplant, which diverged over 15 million years ago [41]. We successfully hybridized probes designed for *C. ocellatus* to the chromosomes of congeneric *C. metallicus*, which diverged 18 Mya (Fig. 4A, B). Chromosome indexing was consistent across the two species, indicating the absence of significant chromosomal rearrangements at the mapped regions. These results demonstrate that probes designed for *C. ocellatus* can be reused effectively in other species of the genus, highlighting their potential for chromosome identification, karyotype evolution studies, and genome validation across *Carinascincus* and potentially beyond.

Aligning probes in silico to other available skink assemblies showed that sequence homology decreases with increasing evolutionary distance. Mapping rates of 10% in *Cryptoblepharus egeriae* (43 million years of divergence) and 2% in *Tiliqua scincoides* (75 million years) indicate that these two species are probably too divergent for effective use of *C. ocellatus* Oligo-FISH probes. *Tiliqua scincoides* belongs to the same subfamily as *L. whitii*, so these results are in line with the lack of hybridization signals in the latter. These in silico alignments did nevertheless reveal that probes still cluster in specific regions across the different genomes (Fig. 4C), suggesting that synteny at the megabase scale is conserved in these skinks. These alignments also

further demonstrate that synteny at the chromosomal level is preserved, particularly for macrochromosomes. Chromosome 3 of *C. ocellatus* and *T. scincoides* exhibits collinearity, aligning with three separate contigs of *C. egeriae* (Ceg5, Ceg6, and Ceg18), a pattern that also holds for chromosome 8 (Ceg12, Ceg14, and Ceg21) (Fig. 4). These two contig triplets presumably represent segments of two incompletely assembled chromosomes in *C. egeriae*, which has not been characterized at the chromosomal level [52]. Synteny is not perfectly conserved in microchromosomes, with a lack of total collinearity within certain chromosomes (e.g., *C. ocellatus* chromosome 13 and *C. egeriae* chromosome 15), or only partial synteny, with segments from a chromosome in one species aligning to multiple chromosomes in another species (e.g., *C. ocellatus* chromosome 10 aligning to *C. egeriae* contig 11 and to *T. scincoides* chromosomes 13 and 16). These discrepancies represent either chromosomal rearrangements that occurred since their lineages diverged or assembly errors. These possibilities are unlikely to be distinguished by in situ hybridization of the *C. ocellatus* oligo probes to metaphases of these two other species given their poor alignment rate to their genomes in silico. The taxonomic scope of probe sets could be increased if multiple reference genomes (chromosome-level assembly or not) are available and used for probe design, by identifying sequences that are shared among them. Overall, the combination of in situ hybridization and in silico alignment of oligo probes offers a promising approach for detecting chromosomal rearrangements and exploring patterns of chromosome evolution across taxa.

Conclusions

The high-quality chromosome-level genome assembly for the Tasmanian spotted snow skink addresses a critical genomic gap for Scincidae, one of the most diverse squamate reptile groups. Combining long-read sequencing, Hi-C scaffolding, and cytogenetic validation, this assembly provides a robust and accurate resource for further evolutionary and functional studies, while also supporting comparative genomics across reptiles.

By integrating Oligo-FISH chromosome indexing, we demonstrate an effective approach for external validation of chromosome models, particularly useful for resolving ambiguous Hi-C signals associated with microchromosomes, common in non-mammalian vertebrates. This method offers a reliable solution for improving accuracy in genome assemblies prone to challenges, such as high repeat content or polyploidy, further enhancing their applicability for downstream analyses.

Methods

Sample collection and sequencing

All spotted snow skinks used in this study were captured on Tasmania's Central Plateau, in the same locality (41 51′S, 146 34′E) and sacrificed following methods approved by the University of Tasmania Animal Ethics Committee (cervical dislocation followed by pithing; Approval A23626). For PacBio Hifi sequencing, blood was collected from a single male, and high molecular weight DNA was extracted using Circulomics Nanobind big DNA kit. For Hi-C, kidneys were collected from a different male (due to multiple extraction and library preparation failures) and snap-frozen. For RNA sequencing (used for genome annotation), brains, gonads, and livers were collected from three other males and three females. Tissues were snap-frozen in liquid nitrogen, and mRNA was extracted at the Garvan Institute.

Extracted blood DNA was shipped to the Australian Genome Research Facility (AGRF) for PacBio HiFi library preparation and sequencing with PacBio Sequel II SMRT Cells. Sequencing yielded 55.15 Gbp of Hifi long read data on two cells (4.42 million reads, with a mean read length of 12.4 kbp). Kidneys were shipped to Biomolecular Resource Facility at the Australian National University (ANU) for Hi-C library preparation using the Arima Hi-C kit, and sequencing was performed on an Illumina Novaseq 6000, producing 197 million read pairs (2*150 nt). For liver RNA, strand-specific RNA-seq libraries were generated and sequenced at the Ramaciotti Centre for Genomics, producing 127–185 86 million 100 nt paired-end reads per sample. Brains and gonads RNA were sequenced previously, following the same procedure [56].

Reference genome assembly

The long read data quality was checked using *Jellyfish* (v2.3.1) [57] with a k-mer size of 35, revealing a low duplication rate (0.07%) and heterozygosity (0.4%). These reads were assembled into contigs using *Hifiasm* (v 0.19.8-r603) [58] with the option –min-hist-cnt 2. The completeness and duplication rate of the primary contig assembly was assessed using *BUSCO* (v5.2.2) [59].

We used the *3D-DNA* pipeline (v180419) [60] to join the contigs into chromosomes. *Juicer* (v1.6) [61] was used to map Hi-C reads to primary contigs, and scaffolding was performed using the *run-asm-pipeline.sh* script provided with the *3D-DNA* package. Different parameters sets were used, based on recommendations from the authors of the program made online (including default; -i 1,000,000 -e -editor-coarse-resolution 100,000 –editor-saturation-centile 40; -i 1,000,000 –editor-coarse-resolution 100,000 –editor-repeat-coverage 10 –editor-coarse-region 500,000; -i 1,000,000 -e

–editor-repeat-coverage 5 –splitter-coarse-stringency 30). In all cases, the resulting candidate assemblies (*.final.hic and *.final.assembly) were unsatisfactory, typically yielding too few or too many candidate chromosome models. In addition, the polish and split steps introduced thousands of breaks, fragmenting many contigs and assigning a substantial proportion of the resulting fragments (several percent of the whole genome) to the list of debris sequences, despite many fragments showing clear and unique Hi-C contacts to surrounding sequences (upon visualization in Juicebox). To address this, we bypassed automated refinement steps and based manual curation on the initial output files (*0.hic and *0.assembly). The Hi-C contact map was visualized in Juicebox, and chromosome boundaries were manually defined, guided by prior knowledge of chromosome number ($n=15$). During this process, four misplaced contigs were moved to appropriate location, and 29 small contigs (0.01 to 0.46 Mbp) with very few contacts were considered as unplaced.

We assembled the mitochondrial genome from the PacBio Hifi reads using *MitoHifi* (v3.2.1) [62]. The script *findMitoReference.py* was used to retrieve the closest available mitochondrial genome (the Sikkim ground skink *Asymblepharus sikimmensis*), which was used as an input to guide mitochondrial read discovery. The final mitochondrial contig (17,866 bp) was blasted against the whole genome to search for high-identity mitochondrial contaminants (>0.95 identity and >500 bp). One unassigned contig (30,806 bp) was removed from the assembly, and 9310 bp were trimmed from chromosome model 2.

Note that despite knowing that chromosome pair 7 is the sex chromosome pair in *C. ocellatus* (homomorphic XY system; [48]), we did not attempt to phase or separately assemble the X and Y chromosomes. The sex chromosome pair is referred to as chromosome 7 in the assembly, and most likely represents a mosaic of the X and Y haplotypes.

Repeat and gene annotation

RepeatModeler (v2.0.5) [63] was used to identify the repeat content in the whole assembled genome. Repetitive regions were annotated and masked in the assembly using *RepeatMasker* (v4.16) [64]. *RepeatMasker's* output was scanned to identify telomeric regions (i.e., containing the telomere hexamer sequence TTAGGG) across all chromosomes and unplaced sequences.

Genes were annotated on a softmasked version of the genome using *BRAKER3* (v3.0.8) [65] which relies on protein and RNAseq data for training to discover gene models. We used the OrthoDB v11 vertebrata protein database [66], and a subset of 50 million RNAseq read pairs from *C. ocellatus* (male and female brain, gonads, and liver) mapped to the genome using *STAR* (v2.7.11) [67] with option –outSAMstrandField intronMotif. *BRAKER3* was performed with options –eptmode and –softmasking. To identify the most confident predictions, we ran the selectSupportedSubsets.py script (provided with *BRAKER3*) to identify those genes/transcripts with external (protein and RNA) support. The script separates gene predictions in three classes: (i) *fully supported genes*, for which start and stop codons, as well as transcripts and introns start and end, are supported by protein and/or RNAseq data, (ii) *partially supported genes*, for which at least one of the previous features is supported by protein and/or RNA hints, (iii) ab initio *no support* genes that are likely false positives. Completeness of the annotation was assessed using *BUSCO* v5.2.2 [59] in protein mode, on the longest isoform of each gene model. Gene functional annotation was performed using *eggNOG-mapper* (v2.1.12), which relies on orthology detection to transfer functional information to proteins [68].

Chromosome indexing

Chromosome-specific oligo probes (myTags®, Daicel Arbor Biosciences, Ann Arbor, USA) were designed to index chromosomes. Target regions were chosen along chromosomes, and within each target region unique short sequences (oligos) were identified in silico. Proximate oligos (typically a few thousand) form an "oligo probe," which produces a visual fluorescent signal when simultaneously hybridized to a metaphase spread. Groups of oligo probes spanning different chromosomal regions are synthesized, amplified, and labeled together in a "oligo library." Hybridizing multiple oligo libraries labeled with different fluorochromes allows generating color patterns unique to each chromosome. Detailed protocols and schematics of the probe design process are available on the Daicel Arbor Biosciences website.

For the *C. ocellatus* genome, to be able to distinguish all 15 chromosomes, three oligo libraries were designed in the manufacturer's pipeline. Each library targeted 14–15 specific spots spanning 0.1–0.3 Mbp on all chromosomes (Additional file 2: Table S5). Each chromosome was covered by three spots, one central and two sub-telomeric, separated by at least 5 Mbp to ensure discriminable FISH signals (one spot on chromosome 15). We provided broad 5 Mbp target intervals to the manufacturer, who identified within these interval regions with high densities of unique oligos suitable for synthesis, in which over 1800 oligos were selected (with dTm > 10 °C to avoid hairpin formation). Probes were synthesized and further labeled during synthesis with Atto488-dUTP for green fluorescence, Atto663-dUTP for yellow fluorescence, or Atto550-dUTP for red fluorescence. To confirm

the high specificity of probes, oligos were aligned in silico to the *C. ocellatus* genome assembly using *Blat* (v35) [69] with options -minID = 95 and -stepSize = 5 to guarantee a match length > 20 bp. One single hit was observed for 99% of all oligos.

A blood cell culture was conducted to obtain metaphase mitotic chromosomes following Hill et al. [48]. Chromosome preparations were then dropped into clean glass slides and aged at − 80 °C for 24 h. Next, 1 µL of each of three probes was mixed by pipetting into 17 µL of hybridization mixture (50% formamide, 2 × SSC, 10% SDS, 10% dextran sulfate, and Denhardt's buffer at pH 7.0) and applied to the slides. A coverslip was added, and borders were sealed with cement rubber for 5 min at RT. Denaturation was performed in a Heat plate at 68 °C for 5 min and hybridization occurred in a dark moist chamber at 37 °C for 24 h. After, the coverslip was gently removed, and the slides were washed in 0.4 × SSC/IGEPAL at 60 °C for 2 min. A second wash in 2 × SSC/IGEPAL was conducted at room temperature for 1 min. Slides were dehydrated in ethanol series (70%, 90%, and 100%) for 1 min each and air dried. Finally, 20 µL of VECTASHIELD® Antifade Mounting Medium with DAPI was applied for counterstain and metaphases were captured in a Leica Microsystems Thunder Imaging system. Karyotypes were assembled based on the patterns created by the Oligo-FISH using Adobe Photoshop CC, after the analysis of at least 30 metaphase spreads per species.

Cross-species analyses

The set of probes used for chromosomal indexing in *C. ocellatus* was also applied for comparative cytogenomic investigations using chromosomes from the congeneric metallic snow skink *C. metallicus* and White's skink *Liophilis whitii* (Egerniinae). The FISH procedure was conducted using the same protocol as above but using 48-h hybridization.

Genome assemblies of the Christmas Island blue-tailed skink *Cryptoblepharus egeriae* and the common blue tongue *Tiliqua scincoides* were downloaded from NCBI (GenBank accession numbers: GCA_030015325.1, GCA_035046505.1), and oligo sequences were aligned to both genomes using *Blat* (-minID = 95 and -stepSize = 5). Whole genome alignments between the three genomes were performed using *LastZ* (v1.04, parameters: –gfextend –notransition –chain –gapped –ambiguous = iupac –step = 20 –masking = 10 –format = axt) [70]. Alignments were filtered to keep only reciprocal best alignments using the chain/net procedure (scripts downloaded from https://github.com/ENCODE-DCC/kentUtils/tree/master/src/hg/mouseStuff; [71]).

Abbreviations

BAC	Bacterial Artificial Chromosome
BUSCO	Benchmarking Universal Single-Copy Orthologs
DAPI	4′,6-Diamidino-2-phenylindole
FISH	Fluorescence in situ hybridization
Gbp	Gigabase pairs
Hi-C	High-throughput chromatin conformation capture
kbp	Kilobase pairs
Mbp	Megabase pairs
nt	Nucleotide
PacBio HiFi	Pacific Biosciences High-Fidelity long-read sequencing

Supplementary Information

The online version contains supplementary material available at https://doi.org/10.1186/s12915-025-02402-9.

Additional file 1: Fig. S1 Hi-C contact map following manual chromosome boundary adjustment. Focus on the microchromosomes. Fig. S2 Repeat percentage, GC content, and gene number in 1-Mb windows across all chromosomes of the *Carinascincus ocellatus* genome. Fig. S3 DAPI-stained chromosomes of *Carinascincus ocellatus* used for FISH experiments. Scale bar = 10 µm.

Additional file 2: Table S1 Available skink genome assemblies prior to this study (NCBI genome platform accessed in March 2025), including assembly level (chromosome or scaffold), assembly size, GC%, and when available, associated publication and BUSCO scores. Table S2 Repeat content across the *Carinascincus ocellatus* chromosomes, in windows of 1 Mbp. Table S3 Telomeric sequences detected in the *Carinascincus ocellatus* genome assembly. Table S4 List of annotated genes, including *Augustus* support level, *Orthofinder* orthology type and Orthogroup and *eggNOG*-mapper functional annotation. Table S5 Oligo probe design: list of chromosomal regions where probes were designed. Table S6 Results of *Lastz* whole genome alignments. Table S7 Distribution of oligo sequences mapped in silico to the genomes of *C. ocellatus*, *C. egeriae*, and *T. scincoides*.

Acknowledgements

Computation was performed at the Life Science Compute Cluster of the University of Vienna. We thank Geoffrey While for performing animal euthanasia. This work was supported by the Australian Research Council (ARC grant DP200101406).

Authors' contributions

EW, TE, CPB, OS and MBC conceived the project. PAS performed genome assembly and bioinformatics analyses. FMCS, MBC and TE performed cytogenetics analyses. PAS wrote the original draft. All authors read, contributed and approved the final manuscript.

Funding

This work was supported by the Australian Research Council (ARC grant DP200101406).

Data availability

Sequence data that support the findings of this study have been deposited in the European Nucleotide Archive with the primary accession code PRJEB88809 (PacBio and Hi-C reads; [72]); and NCBI with primary accession code PRJNA975681 (RNAseq reads; [73]). Genome accession number: GCA_965280105.1 [74]. Gene annotation available at https://doi.org/10.5281/zenodo.16539564.

Declarations

Ethics approval and consent to participate

Animal collection, handling, and euthanasia were conducted under approval A23626 from the University of Tasmania Animal Ethics Committee.

Consent for publication
Not applicable.

Competing interests
The authors declare no competing interests.

Author details
[1]School of Natural Sciences, University of Tasmania, Sandy Bay, TAS 7000, Australia. [2]CEFE, Université de Montpellier, CNRS, EPHE, IRD, Montpellier, France. [3]Institute for Applied Ecology, University of Canberra, Bruce, ACT 2601, Australia. [4]School of Life Sciences, Southwest University, Chongqing, China. [5]Laboratory of Evolutionary Cytogenetics, Department of Genetics and Evolution, Universidade Federal de São Carlos, São Carlos 13565-905, SP, Brazil. [6]Department for Neurosciences and Developmental Biology, University of Vienna, 1030 Vienna, Austria.

Received: 16 June 2025 Accepted: 29 August 2025
Published online: 08 October 2025

References

1. Chapple DG, Roll U, Böhm M, Aguilar R, Amey AP, Austin CC, et al. Conservation status of the world's skinks (Scincidae): taxonomic and geographic patterns in extinction risk. Biol Conserv. 2021. https://doi.org/10.1016/j.biocon.2021.109101.
2. Gardner MG, Pearson SK, Johnston GR, Schwarz MP. Group living in squamate reptiles: a review of evidence for stable aggregations. Biol Rev. 2016;91:925–36. https://doi.org/10.1111/brv.12201.
3. While GM, Chapple DG, Gardner MG, Uller T, Whiting MJ. Egernia lizards. Curr Biol. 2015;25:R593–5. https://doi.org/10.1016/j.cub.2015.02.070.
4. Greer AE. Limb reduction in squamates: identification of the lineages and discussion of the trends. J Herpetol. 1991;25:166–73.
5. Van Dyke JU, Thompson MB, Burridge CP, Castelli MA, Clulow S, DIssanayake DSB, et al. Australian lizards are outstanding models for reproductive biology research. Aust J Zool. 2021;68:168–99. https://doi.org/10.1071/ZO21017.
6. Pen I, Uller T, Feldmeyer B, Harts A, While GM, Wapstra E. Climate-driven population divergence in sex-determining systems. Nature. 2010;468:436–8. https://doi.org/10.1038/nature09512.
7. Fitzpatrick LJ, Olsson M, Pauliny A, While GM, Wapstra E. Individual telomere dynamics and their links to life history in a viviparous lizard. Proc R Soc Lond B Biol Sci. 2021;288:20210271. https://doi.org/10.1098/rspb.2021.0271.
8. Cunningham GD, While GM, Olsson M, Ljungström G, Wapstra E. Degrees of change: between and within population variation in thermal reaction norms of phenology in a viviparous lizard. Ecology. 2020;101:e03136. https://doi.org/10.1002/ecy.3136.
9. Hill PL, Burridge CP, Ezaz T, Wapstra E. Conservation of sex-linked markers among conspecific populations of a viviparous skink, *Niveoscincus ocellatus*, exhibiting genetic and temperature-dependent sex determination. Genome Biol Evol. 2018;10:1079–87. https://doi.org/10.1093/gbe/evy042.
10. Simakov O, Bredeson J, Berkoff K, Marletaz F, Mitros T, Schultz DT, et al. Deeply conserved synteny and the evolution of metazoan chromosomes. Sci Adv. 2022;8:eabi5884.
11. Christmas MJ, Goodman DB, Lind AL, Redlich RW, Brown AR, Teeling EC, et al. Evolutionary constraint and innovation across hundreds of placental mammals. Science. 2023;380:eabn3943. https://doi.org/10.1126/SCIENCE.ABN3943.
12. Chen X, Wang Z, Zhang C, Hu J, Lu Y, Zhou H, et al. Unraveling the complex evolutionary history of lepidopteran chromosomes through ancestral chromosome reconstruction and novel chromosome nomenclature. BMC Biol. 2023;21:265. https://doi.org/10.1186/s12915-023-01762-4.
13. Muffato M, Louis A, Nguyen NTT, Lucas J, Berthelot C, Roest Crollius H. Reconstruction of hundreds of reference ancestral genomes across the eukaryotic kingdom. Nat Ecol Evol. 2023;7:355–66. https://doi.org/10.1038/s41559-022-01956-z.
14. Brandies P, Peel E, Hogg CJ, Belov K. The value of reference genomes in the conservation of threatened species. Genes. 2019;10:846. https://doi.org/10.3390/genes10110846.
15. Formenti G, Theissinger K, Fernandes C, Bista I, Bombarely A, Bleidorn C. The era of reference genomes in conservation genomics. Trends Ecol Evol. 2021;37:197–202.
16. Theissinger K, Fernandes C, Formenti G, Bista I, Berg PR, Bleidorn C, et al. How genomics can help biodiversity conservation. Trends Genet. 2023;39:545–59. https://doi.org/10.1016/j.tig.2023.01.005.
17. Wold J, Koepfli KP, Galla SJ, Eccles D, Hogg CJ, Le Lec MF, et al. Expanding the conservation genomics toolbox: incorporating structural variants to enhance genomic studies for species of conservation concern. Mol Ecol. 2021;30:5949–65. https://doi.org/10.1111/mec.16141.
18. Pal K, Forcato M, Ferrari F. Hi-c analysis: from data generation to integration. Biophys Rev. 2019;11:67–78. https://doi.org/10.1007/s12551-018-0489-1.
19. Rhie A, McCarthy SA, Fedrigo O, Damas J, Formenti G, Koren S, et al. Towards complete and error-free genome assemblies of all vertebrate species. Nature. 2021;592:737–46. https://doi.org/10.1038/s41586-021-03451-0.
20. Bringloe TT, Parent GJ. Contrasting new and available reference genomes to highlight uncertainties in assemblies and areas for future improvement: an example with monodontid species. BMC Genomics. 2023;24:693. https://doi.org/10.1186/s12864-023-09779-3.
21. Kadota M, Nishimura O, Miura H, Tanaka K, Hiratani I, Kuraku S. Multifaceted Hi-C benchmarking: what makes a difference in chromosome-scale genome scaffolding? Gigascience. 2020;9:1–15. https://doi.org/10.1093/gigascience/giz158.
22. Yamaguchi K, Kadota M, Nishimura O, Ohishi Y, Naito Y, Kuraku S. Technical considerations in Hi-C scaffolding and evaluation of chromosome-scale genome assemblies. Mol Ecol. 2021;30:5923–34. https://doi.org/10.1111/mec.16146.
23. Perry BW, Schield DR, Adams RH, Castoe TA. Microchromosomes exhibit distinct features of vertebrate chromosome structure and function with underappreciated ramifications for genome evolution. Mol Biol Evol. 2021;38:904–10. https://doi.org/10.1093/molbev/msaa253.
24. Waters PD, Patel HR, Ruiz-Herrera A, Alvarez-Gonzalez L, Lister NC, Simakov O, et al. Microchromosomes are building blocks of bird, reptile, and mammal chromosomes. Proc Natl Acad Sci U S A. 2021;118:1–11. https://doi.org/10.1073/pnas.2112494118.
25. Davalos-Dehullu E, Baty SM, Fisher RN, Scott PA, Dolby GA, Munguia-Vega A, et al. Chromosome-level genome assembly of the blacktail brush lizard, *Urosaurus nigricaudus*, reveals dosage compensation in an endemic lizard. Genome Biol Evol. 2023;15:evad210. https://doi.org/10.1093/gbe/evad210.
26. Luo H, Jiang X, Li B, Wu J, Shen J, Xu Z, et al. A high-quality genome assembly highlights the evolutionary history of the great bustard (*Otis tarda*, Otidiformes). Commun Biol. 2023;6:746. https://doi.org/10.1038/s42003-023-05137-x.
27. Schield DR, Card DC, Hales NR, Perry BW, Pasquesi GM, Blackmon H, et al. The origins and evolution of chromosomes, dosage compensation, and mechanisms underlying venom regulation in snakes. Genome Res. 2019;29:590–601. https://doi.org/10.1101/gr.240952.118.
28. Lewin HA, Graves JAM, Ryder OA, Graphodatsky AS, O'Brien SJ. Precision nomenclature for the new genomics. GigaScience. 2019;8:giz086. https://doi.org/10.1093/gigascience/giz086.
29. Shi Y, Chen B, Kong S, Zeng Q, Li L, Liu B, et al. Comparative genomics analysis and genome assembly integration with the recombination landscape contribute to *Takifugu bimaculatus* assembly refinement. Gene. 2023;849:146910. https://doi.org/10.1016/j.gene.2022.146910.
30. Koochekian N, Ascanio A, Farleigh K, Card DC, Schield DR, Castoe TA, et al. A chromosome-level genome assembly and annotation of the desert horned lizard, *Phrynosoma platyrhinos*, provides insight into chromosomal rearrangements among reptiles. Gigascience. 2022;11:giab098. https://doi.org/10.1093/gigascience/giab098.
31. Uno Y, Nozu R, Kiyatake I, Higashiguchi N, Sodeyama S, Murakumo K, et al. Cell culture-based karyotyping of orectolobiform sharks for chromosome-scale genome analysis. Commun Biol. 2020;3:652. https://doi.org/10.1038/s42003-020-01373-7.
32. Shearer LA, Anderson LK, de Jong H, Smit S, Goicoechea JL, Roe BA, et al. Fluorescence in situ hybridization and optical mapping to correct scaffold arrangement in the tomato genome. G3 Genes|Genomes|Genetics. 2014;4:1395–405. https://doi.org/10.1534/g3.114.011197.

33. Iannucci A, Makunin AI, Lisachov AP, Ciofi C, Stanyon R, Svartman M, et al. Bridging the gap between vertebrate cytogenetics and genomics with single-chromosome sequencing (ChromSeq). Genes. 2021;12:124. https://doi.org/10.3390/genes12010124.
34. Zwyrtková J, Šimková H, Doležel J. Chromosome genomics uncovers plant genome organization and function. Biotechnol Adv. 2021;46:107659. https://doi.org/10.1016/j.biotechadv.2020.107659.
35. Fierst JL. Using linkage maps to correct and scaffold de novo genome assemblies: methods, challenges, and computational tools. Front Genet. 2015;6:220. https://doi.org/10.3389/fgene.2015.00220.
36. Rice ES, Green RE. New approaches for genome assembly and scaffolding. Annu Rev Anim Biosci. 2019;7:17–40. https://doi.org/10.1146/annurev-animal-020518-115344.
37. Damas J, O'Connor R, Farré M, Lenis VPE, Martell HJ, Mandawala A, et al. Upgrading short-read animal genome assemblies to chromosome level using comparative genomics and a universal probe set. Genome Res. 2017;27:875–84. https://doi.org/10.1101/gr.213660.116.
38. O'Connor RE, Farré M, Joseph S, Damas J, Kiazim L, Jennings R, et al. Chromosome-level assembly reveals extensive rearrangement in saker falcon and budgerigar, but not ostrich, genomes. Genome Biol. 2018. https://doi.org/10.1186/s13059-018-1550-x.
39. Beliveau BJ, Joyce EF, Apostolopoulos N, Yilmaz F, Fonseka CY, McCole RB, et al. Versatile design and synthesis platform for visualizing genomes with Oligopaint FISH probes. Proc Natl Acad Sci U S A. 2012;109:21301–6. https://doi.org/10.1073/pnas.1213818110.
40. Han Y, Zhang T, Thammapichai P, Weng Y, Jiang J. Chromosome-specific painting in *Cucumis* species using bulked oligonucleotides. Genetics. 2015;200:771–9. https://doi.org/10.1534/genetics.115.177642.
41. Braz GT, He L, Zhao H, Zhang T, Semrau K, Rouillard JM, et al. Comparative oligo-FISH mapping: an efficient and powerful methodology to reveal karyotypic and chromosomal evolution. Genetics. 2018;208:513–23. https://doi.org/10.1534/genetics.117.300344.
42. He L, Braz GT, Torres GA, Jiang J. Chromosome painting in meiosis reveals pairing of specific chromosomes in polyploid *Solanum* species. Chromosoma. 2018;127:505–13. https://doi.org/10.1007/s00412-018-0682-9.
43. He L, Zhao H, He J, Yang Z, Guan B, Chen K, et al. Extraordinarily conserved chromosomal synteny of *Citrus* species revealed by chromosome-specific painting. Plant J. 2020;103:2225–35. https://doi.org/10.1111/tpj.14894.
44. Bielski W, Książkiewicz M, Šimoníková D, Hřibová E, Susek K, Naganowska B. The puzzling fate of a lupin chromosome revealed by reciprocal oligo-fish and bac-fish mapping. Genes. 2020;11:1–17. https://doi.org/10.3390/genes11121489.
45. Huang Z. Evolutionary analysis of a complete chicken genome. Proc Natl Acad Sci. 2023;120:e2216641120. https://doi.org/10.1073/pnas.
46. Poisson W, Prunier J, Carrier A, Gilbert I, Mastromonaco G, Albert V, et al. Chromosome-level assembly of the *Rangifer tarandus* genome and validation of cervid and bovid evolution insights. BMC Genomics. 2023;24:1–17. https://doi.org/10.1186/s12864-023-09189-5.
47. Donnellan SC. The evolution of sex chromosomes in scincid lizards. Sydney, NSW, Australia: Macquarie University; 1985.
48. Hill P, Shams F, Burridge CP, Wapstra E, Ezaz T. Differences in homomorphic sex chromosomes are associated with population divergence in sex determination in *Carinascincus ocellatus* (Scincidae: Lygosominae). Cells. 2021;10:291.
49. Hanrahan BJ, Alreja K, Reis ALM, Chang JK, Dissanayake DSB, Edwards RJ, et al. A genome assembly and annotation for the Australian alpine skink *Bassiana duperreyi* using long-read technologies. G3 Genes Genomes Genet. 2025;15:jkaf046. https://doi.org/10.1093/g3journal/jkaf046.
50. Rivera D, Henderson JB, Lam AW, Hostetter NJ, Collazo JA, Bell RC. High-quality, chromosome-level reference genomes of the viviparous Caribbean skinks Spondylurus nitidus and S. culebrae. Genome Biol Evol. 2024;16:1–7. https://doi.org/10.1093/gbe/evae079.
51. Deakin JE, Potter S, O'neill R, Ruiz-Herrera A, Cioffi MB, Eldridge MDB, et al. Chromosomics: bridging the gap between genomes and chromosomes. Genes. 2019;10(8):627. https://doi.org/10.3390/genes10080627.
52. Dodge TO, Farquharson KA, Ford C, Cavanagh L, Schubert K, Schumer M, et al. Genomes of two extinct-in-the-wild reptiles from Christmas Island reveal distinct evolutionary histories and conservation insights. Mol Ecol Resour. 2022;2023:1–17. https://doi.org/10.1111/1755-0998.13780.
53. Deakin JE, Ezaz T. Understanding the evolution of reptile chromosomes through applications of combined cytogenetics and genomics approaches. Cytogenet Genome Res. 2019;157:7–20. https://doi.org/10.1159/000495974.
54. Bourke PM, Van Geest G, Voorrips RE, Jansen J, Kranenburg T, Shahin A, et al. PolymapR - linkage analysis and genetic map construction from F 1 populations of outcrossing polyploids. Bioinformatics. 2018;34:3496–502. https://doi.org/10.1093/bioinformatics/bty371.
55. Grandke F, Ranganathan S, van Bers N, de Haan JR, Metzler D. PERGOLA: fast and deterministic linkage mapping of polyploids. BMC Bioinformatics. 2017;18:1–9. https://doi.org/10.1186/s12859-016-1416-8.
56. Saunders PA, Ferre-Ortega C, Hill PL, Simakov O, Ezaz T, Burridge CP, et al. Using a handful of transcriptomes to detect sex-linked markers and develop molecular sexing assays in a species with homomorphic sex chromosomes. Genome Biol Evol. 2024;16:1–7. https://doi.org/10.1093/gbe/evae060.
57. Marçais G, Kingsford C. A fast, lock-free approach for efficient parallel counting of occurrences of k-mers. Bioinformatics. 2011;27:764–70. https://doi.org/10.1093/bioinformatics/btr011.
58. Cheng H, Concepcion GT, Feng X, Zhang H, Li H. Haplotype-resolved de novo assembly using phased assembly graphs with hifiasm. Nat Methods. 2021;176:170–5. https://doi.org/10.1038/s41592-020-01056-5.
59. Manni M, Berkeley MR, Seppey M, Simão FA, Zdobnov EM. BUSCO update: novel and streamlined workflows along with broader and deeper phylogenetic coverage for scoring of eukaryotic, prokaryotic, and viral genomes. Mol Biol Evol. 2021;38:4647–54. https://doi.org/10.1093/molbev/msab199.
60. Dudchenko O, Batra SS, Omer AD, Nyquist SK, Hoeger M, Durand NC, et al. De novo assembly of the *Aedes aegypti* genome using Hi-C yields chromosome-length scaffolds. Science. 2017;356:92–5. https://doi.org/10.1126/science.aal3327.
61. Durand NC, Shamim MS, Machol I, Rao SSP, Huntley MH, Lander ES, et al. Juicer provides a one-click system for analyzing loop-resolution Hi-C experiments. Cell Syst. 2016;3:95–8. https://doi.org/10.1016/j.cels.2016.07.002.
62. Uliano-Silva M, Ferreira JGRN, Krasheninnikova K, Blaxter M, Mieszkowska N, Hall N, et al. MitoHiFi: a python pipeline for mitochondrial genome assembly from PacBio high fidelity reads. BMC Bioinformatics. 2023;24:1–13. https://doi.org/10.1186/s12859-023-05385-y.
63. Flynn JM, Hubley R, Goubert C, Rosen J, Clark AG, Feschotte C, et al. Repeatmodeler2 for automated genomic discovery of transposable element families. Proc Natl Acad Sci U S A. 2020. https://doi.org/10.1073/pnas.1921046117.
64. Smit AFA, Hubley R, Green P. RepeatMasker Open-4.0. 2015. http://www.repeatmasker.org. Accessed 01 May 2024.
65. Gabriel L, Brůna T, Hoff KJ, Ebel M, Lomsadze A, Borodovsky M, et al. BRAKER3: fully automated genome annotation using RNA-seq and protein evidence with GeneMark-ETP, AUGUSTUS, and TSEBRA. Genome Res. 2024;34:769–77. https://doi.org/10.1101/gr.278090.123.
66. Kuznetsov D, Tegenfeldt F, Manni M, Seppey M, Berkeley M, Kriventseva EV, et al. OrthoDB v11: annotation of orthologs in the widest sampling of organismal diversity. Nucleic Acids Res. 2023;51(D1):D445-51. https://doi.org/10.1093/nar/gkac998.
67. Dobin A, Davis CA, Schlesinger F, Drenkow J, Zaleski C, Jha S, et al. STAR: ultrafast universal RNA-seq aligner. Bioinformatics. 2013;29:15–21. https://doi.org/10.1093/bioinformatics/bts635.
68. Cantalapiedra CP, Hernández-Plaza A, Letunic I, Bork P, Huerta-Cepas J. eggNOG-mapper v2: Functional Annotation, Orthology Assignments, and Domain Prediction at the Metagenomic Scale. Mol Biol Evol. 2021;38:5825–9. https://doi.org/10.1093/molbev/msab293.
69. Kent WJ. BLAT—the BLAST-like alignment tool. Genome Res. 2002;12:656–64. https://doi.org/10.1101/gr.229202.
70. Harris RS. Improved pairwise alignment of genomic DNA. The Pennsylvania State University. 2007. Accessible at: https://www.proquest.com/openview/bc77cca0fb9390b44b9ef572fb574322/1?pq-origsite=gscholar&cbl=18750.
71. Kent WJ, Baertsch R, Hinrichs A, Miller W, Haussler D. Evolution's cauldron: duplication, deletion, and rearrangement in the mouse and human genomes. Proc Natl Acad Sci U S A. 2003;100:11484–9. https://doi.org/10.1073/pnas.1932072100.

72. Chromosome-level assembly for *Carinascincus ocellatus*, ENA Bioproject accession: PRJEB88809. 2025.
73. Spotted snow skink RNAseq, NCBI Bioproject accession: PRJNA975681. 2023.
74. Chromosome-level assembly (PacBio HiFi + HiC) for the Tasmanian spotted snow skink *Carinascincus ocellatus*, accession number: GCA_965280105.1. 2025.
75. Hedges SB. The high-level classification of skinks (Reptilia, Squamata, Scincomorpha). Zootaxa. 2014;3765:317–38. https://doi.org/10.11646/zootaxa.3765.4.2.
76. Uetz P, Koo MS, Aguilar R, Brings E, Catenazzi A, Chang AT, et al. A quarter century of reptile and amphibian databases. Herpetol Rev. 2021;52:246–55.

Publisher's Note